Water Practice & Technology

Water Practice & Technology Vol 18 No 7, 1628 doi: 10.2166/wpt.2023.097

Fixed-bed column sorption kinetic rates on the removal of both biochemical oxygen demand (BOD_5) and chemical oxygen demand (COD) in domestic greywater by using palm kernel activated carbon

Michael Oteng-Peprah[a,*], Peter Appiah Obeng[a], Mike Agbesi Acheampong[b] and Michael Akrofi Anang[c]

[a] Department of Water and Sanitation, University of Cape Coast, Cape Coast, Ghana
[b] Department of Chemical Engineering, Kumasi Technical University, Kumasi, Ghana
[c] Department of Chemistry, Industrial Chemistry Unit, University of Cape Coast, Cape Coast, Ghana
*Corresponding author. E-mail: moteng-peprah@ucc.edu.gh

MO, 0000-0002-8301-2300

ABSTRACT

The increasing organic loads, specifically biochemical oxygen demand (BOD_5) and chemical oxygen demand (COD), in water bodies has necessitated greywater treatment before disposal. Limited studies have explored sorption kinetics of BOD_5 and COD removal using activated carbon from palm kernel shell in fixed-bed columns. This study investigated continuous sorption using activated carbon from palm kernel in removing BOD_5 and COD from domestic greywater. The activated carbon had a density of 0.46 g cm^{-3} and a surface area of 584 m^2 g^{-1}. The experiment was conducted in a 37 cm high, 2.5 cm diameter Perspex column, with varying flowrates of 5–15 mL min^{-1}, and bed depths of 10, 15, and 20 cm. Greywater with BOD_5 concentration of 251 mg L^{-1} and COD of 421 mg L^{-1} was used for this study. Effluent was collected at specified time intervals, analyzed for BOD_5 and COD, and fitted to the Thomas, Yoon–Nelson, Adams–Bohart, and Bed Depth Service Time (BDST) models. The Yoon–Nelson model exhibited good agreement, as compared to Thomas and BDST while the Adams–Bohart model showed lower fit. The adsorbent demonstrated sorption capacities of 34 mg g^{-1} for BOD_5 and 56 mg g^{-1} for COD, suggesting its potential for greywater treatment, particularly in BOD_5 and COD removal.

Key words: activated carbon, biochemical oxygen demand, chemical oxygen demand, fixed-bed column, palm kernel

HIGHLIGHTS

- The research explored the use of palm kernel activated carbon in a column experiment to reduce BOD and COD in domestic grey water.
- No research has explored this reduction in a column experiment.
- Adsorption data were fitted to the column models.
- The research established that it is possible to reduce BOD and COD to acceptable levels using a local waste material.
- Using waste materials is environmentally beneficial.

1. INTRODUCTION

Increasing concerns regarding the impact of untreated greywater on the environment have prompted the need for stricter environmental regulations governing the discharge of both industrial and domestic wastewater. Greywater, which can differ in both volume and quality, is influenced by various factors. It has been noted that the composition of greywater is influenced by elements such as cooking and cleaning methods, personal hygiene habits, biodegradability, frequency of water usage prior to disposal, and sanitary practices (Oteng-Peprah *et al.* 2018). Over the past few decades, growing recognition of the ecological consequences associated with organic loads has resulted in heightened requests for the treatment of greywater before it is released into natural bodies of water (Kurniawan *et al.* 2021). Of particular interest is the concentration of BOD_5 and COD in greywater discharged into the environment. High levels of BOD_5 and COD in water can lead to oxygen depletion, altered ecosystem balance, nutrient imbalance and impaired water quality (Ademiluyi *et al.* 2009; Alewi *et al.* 2021). These can lead to pollution and may have detrimental effect on aquatic life and water quality. The Ghana Environmental Protection

Agency (Ghana. 2000) has set the limit for the concentration of the discharge of BOD_5 and COD at 50 mg L^{-1} and 150 mg L^{-1} respectively. However, wastewater discharged into the environment are mostly above this regulatory limit. To meet the discharge guidelines, greywater from households and industrial settings will require an appreciable level of treatment. Chemical, biological, and physical methods are the conventional approaches employed to treat wastewater containing organic substances. Among the various physico-chemical processes utilized in wastewater treatment, adsorption techniques have emerged as the most extensively employed and effective means (Patel *et al.* 2021). One of the most efficient and simple methods for removal of BOD_5 and COD from greywater is adsorption which is much preferred due to its ease of use and wide-scale application. This technique is quite popular due to its simplicity as well as the availability of a wide range of adsorbents. Activated carbon remains one of the most widely used range of adsorbents. It remains one of the most effective and widely used adsorbents because of its excellent adsorption ability (Mohammad-Khah & Ansari 2009). It has been prepared from many substrates over the years, however, commercial grade activated carbon comes with a higher price tag as compared to those prepared with low-cost materials (Bulut *et al.* 2007; Errais *et al.* 2011; Sartape *et al.* 2013; Nayl *et al.* 2017). Batch adsorption experimental designs are the most commonly utilized tests by many researchers in assessing the suitability of potential adsorbents because of its simplicity and low cost (Crini *et al.* 2008). Data obtained from batch studies are usually used to construct isotherms which are considered a critical step in the design and optimization of the adsorption process (Hamdaoui & Naffrechoux 2007; Behnamfard & Salarirad 2009). Many studies have reported removal of BOD_5 and COD in batch systems using various adsorbents (Bansode *et al.* 2004; Devi *et al.* 2008; Nayl *et al.* 2017) but little has been known on the removal of BOD_5 and COD in a fixed-bed column application. Of particular interest is the batch study by Oteng-Peprah *et al.* (2019) which reported BOD_5 and COD removal from domestic greywater using activated carbon prepared from palm kernel shell. It has been reported that the data obtained under batch conditions are generally not applicable in most systems or do not mimic what happens in the real world (Patel & Vashi 2012). Therefore, in order to validate the data obtained in this batch study there is the need to perform column studies to provide data for direct application to large scale use. There exist many studies that have assessed batch and column studies of many contaminants in wastewater. However, little has been known on column study on greywater targeting the continuous removal of BOD and COD. The aim of this study is therefore to investigate the adsorption capacity of the Palm Kernel Activated Carbon (PKAC) in a fixed-bed column with regards to BOD_5 and COD removal. The PKAC investigated in this study has previously been shown to be effective in removing BOD_5 and COD from greywater in a previous study under batch conditions (Oteng-Peprah *et al.* 2019). The breakthrough curves are analyzed using Adams–Bohart, Thomas, Yoon–Nelson and the BDST models to determine the characteristic parameters of the column useful for process design.

1.1. Column adsorption model

To design a column adsorption process, it is important to predict the breakthrough curve or concentration-like profile and adsorption capacity of the adsorbent for the selected adsorbate under a given set of operating conditions. It is also necessary to determine the maximum sorption column capacity which is a significant parameter for any sorption system. For analysis of the experimental breakthrough curves under different conditions, these common models were used, thus, the Thomas, Yoon–Nelson, Adams–Bohart models and the bed-depth service time (BDST) model.

1.1.1. The Thomas model

The Thomas model (Thomas 1944) is one of the most general and widely used models in column performance theory. It is based on the assumption that the process follows Langmuir kinetics with no axial dispersion and the rate driving force follows second order reversible kinetics (Futalan *et al.* 2011). It is represented by Equation (1) as shown:

$$\ln\left(\frac{C_o}{C_i} - 1\right) = \frac{k_{Th} q_o w}{Q} - k_{Th} C_o t \tag{1}$$

where k_{Th} is the Thomas rate constant (mL min^{-1} mg^{-1}) q_o is the maximum solid-phase concentration of solute (mg g^{-1}); w is the mass of the adsorbent in the column (g); Q is the flow rate (ml min^{-1}); C_i is effluent concentration (mg L^{-1}) and C_o is the influent concentration (mg L^{-1}).

A plot of *ln(C*$_o$*/C*$_t$ *– 1)* against *t* gives a straight line from which the values of k_{Th} and q_o are determined from the intercept and the slope respectively.

1.1.2. Adams–Bohart

This model assumes that the adsorption rate is proportional to both the residual capacity of the adsorbent and the concentration of the adsorbing species. The model is mostly used for the description of the initial part of the breakthrough curve (Han *et al.* 2008). It is expressed by Equation (2) as shown:

$$\ln\left(\frac{C_o}{C_t}-1\right)=k_{AB}N_o\frac{z}{u}-k_{AB}C_t t \tag{2}$$

where C_t is the effluent concentration (mg L^{-1}), C_o is the influent concentration (mg L^{-1}), $\mathrm{k_{AB}}$ is the kinetic constant (L mg^{-1} min^{-1}), N_o is the sorption capacity (mg L^{-1}), Z is the bed-depth (cm), u the linear velocity (mmh^{-1}) and t is the time (h).

A plot of *ln(C*$_o$*/C*$_t$ *– 1)* against *t* gives a straight line from which the model constants k_{AB} and N_o can be determined from the slope and intercept.

1.1.3. Yoon–Nelson

This model is based on the assumption that the rate of decrease in the probability of adsorption for each adsorbate molecule is proportional to the probability of adsorbate adsorption and the probability of adsorbate breakthrough on the adsorbent (Han *et al.* 2008). This model is less complicated and requires no detailed data concerning the characteristics of sorbate, the type of adsorbent and the physical properties of the sorption bed (Yoon & Nelson 1984). It is expressed by Equation (3) as shown:

$$\ln\left(\frac{C_t}{C_o-C_t}\right)= K_{YN}t-\tau K_{YN} \tag{3}$$

where C_t is the effluent concentration (mg L^{-1}), C_o is the influent concentration (mg L^{-1}), K_{YN} is the rate constant (min^{-1}), τ the time required for 50% sorbate breakthrough and t is the time (min).

A linear plot of *ln(C*$_t$*/C*$_O$*-C*$_t$*)* against time t gives a straight line where K_{YN} and τ are determined from the intercept and slope.

1.1.4. Bed depth service time (BDST)

This is a simple semiempirical model used in fixed-bed analysis to predict the performance of an adsorbent. It is based on the assumption that the rate of adsorption is controlled by surface reaction between the adsorbate and the unused capacity of the adsorbent (Han *et al.* 2008; Singha & Sarkar 2015). It is expressed by Equations (4) and (5) as:

$$t=\frac{N_o}{C_oF}Z-\frac{1}{K_oC_o}\ln\left(\frac{C_o}{C_i}-1\right) \tag{4}$$

A plot of t versus bed-depth Z gives a straight line from where N_o and K_o can be evaluated from the slope and intercept respectively

$$Z_o=\frac{F}{K_aN_o}\ln\left(\frac{C_o}{C_i}-1\right) \tag{5}$$

where C_i is the effluent concentration (mg L^{-1}), C_o is the influent concentration (mg L^{-1}), Z_o is the critical bed-depth, K_o is the rate constant, Z is the bed-depth (cm), F is the vertical velocity (cm min^{-1}).

2. METHODOLOGY

2.1. Greywater samples

Greywater for this experiment was obtained from domestic sources within University of Cape Coast community, Ghana.

The samples were stored, refrigerated and transported to the laboratory in an ice chest after the field parameters were analysed onsite. The greywater was filtered to remove large and floating objects and their initial concentrations determined. The pH was determined using a Horiba U-50 multiparameter water quality meter; the BOD_5 was measured using the Lovibond BD 606 system, and the concentration of chemical oxygen demand (COD) was determined using the closed reflux colorimetric method as stated in (APHA) 5220D. To ensure quality assurance, blank sample was prepared using 50 mL of distilled water and treating it with the same reagents for both BOD_5 and COD analysis.

2.2. Material processing

The palm kernel shell was obtained from a local palm oil mill in Cape Coast Ghana. The material is cleaned several times with distilled water to eliminate any dirt and water-soluble impurities. The cleaned shells were then airdried in a laboratory drier for 8 hours and then further oven dried at 110 °C in a Heratherm gravity convection laboratory oven for 24 hours in order to remove any surface moisture. The dried samples were then size reduced to desired sizes (2–6 mm) using a laboratory crusher and sieves. The activated carbons were prepared by physical activation with steam at 800 °C and steam flowrate at 120 mL hr^{-1}. After the activation process, the samples were taken out and washed with distilled water to remove any residual ash that might be on the carbons.

The density of the materials was determined by using an ultra-pycnometer 1000 after it had been dried at 105 °C in an oven for 24 hours. The surface area Brunauer–Emmet–Teller S_{BET} was determined using a Micromeritics tristar 3000 system.

2.3. Fixed-bed column experiments

The fixed-bed column experiments were carried out to assess the performance of palm kernel activated carbon in removing BOD_5 and COD from greywater. This was conducted in a 25 mm inner diameter and 37 cm length Perspex glass column. Palm kernel activated carbon of average particle size of 2 mm was loaded into the Perspex glass column. Glass beads were placed at the bottom of the column to provide support for the adsorbents and placed at the top to prevent the adsorbents from being pulled with the overflow. All experiments were conducted at room temperature with a pH of 7.3 and the direction of flow was from top to bottom using a peristaltic pump. The effluents were collected at regular intervals and the BOD_5 and COD concentrations determined. Flowrate and bed-depth were varied in these experiments. Flowrates of 5, 10 and 15 mL min^{-1} were used to analyze the effect of flowrate variations while bed-depth of 10, 15 and 20 cm were used to analyze the effect of different bed-depth on the column performance. Before the column experiment, deionized water was circulated through the column in order to wet the entire adsorbate and remove any dirt residue on the surface of the carbon.

3. RESULTS AND DISCUSSION

3.1. Physical characteristics of the activated carbon

The apparent density of palm kernel activated carbon (PKAC) was determined to be 0.46 g cm^{-3}. The recommended range of densities for activated carbon is within 0.4–0.5 g cm^{-3} (TIGG 2019) which implies that PKAC falls within the recommended densities for commercial activated carbon. The BET surface area obtained for PKAC was 620 m^2 g^{-1}. The recommended range of surface area of commercial activated carbon has been estimated to be 500–1,500 m^2/g. this shows that the surface area for PKAC falls within the recommended surface area for commercial grade activated carbon. A similar study by Hidayu & Muda (2016) on characterization of activated carbon using palm kernel shell obtained surface area of 584 m^2 g^{-1}. The slight variations in the surface area recorded for this study may be due to the activation method that was used. A higher BET generally suggests higher adsorption capacity because the carbon has wider surface to allow for adsorption under different conditions.

3.2. Effect of flow rate on BOD_5 and COD removal

The effect of BOD_5 and COD removal in a fixed bed column by using three different flowrates was studied. The breakthrough curves obtained at different flowrates (5, 10, 15 mL min^{-1}), constant inlet concentration (BOD_5 = 252 mg L^{-1}, COD = 421 mg L^{-1}) and bed-depth of 20 cm are presented in Figures 1 and 2 respectively. As can be seen from the figures, the breakthrough time, as well as the exhaustion time, increased with decreasing flowrate for both BOD_5 and COD removal. The slopes of these plots show a decrease in duration from breakthrough time to exhaustion time as the flowrate is increased from 5 to 15 mL min^{-1}. This is supported by the increase in the

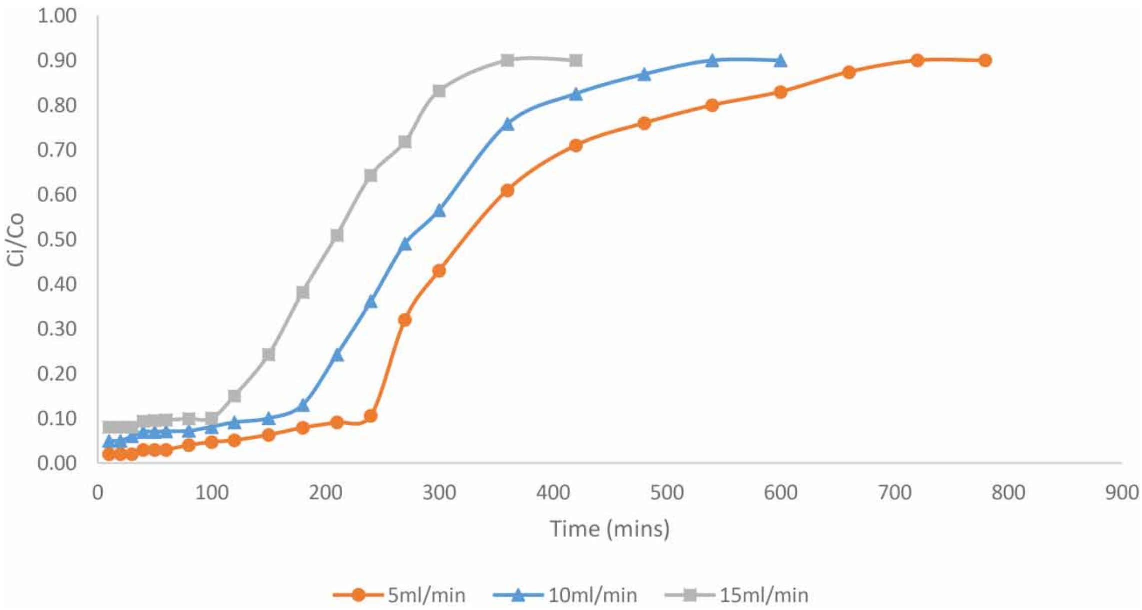

Figure 1 | Breakthrough curves of BOD_5 removal by PKAC (pH = 7.3, bed-depth = 20 cm, temperature = 25 °C, inlet concentration = 252 mg L^{-1}).

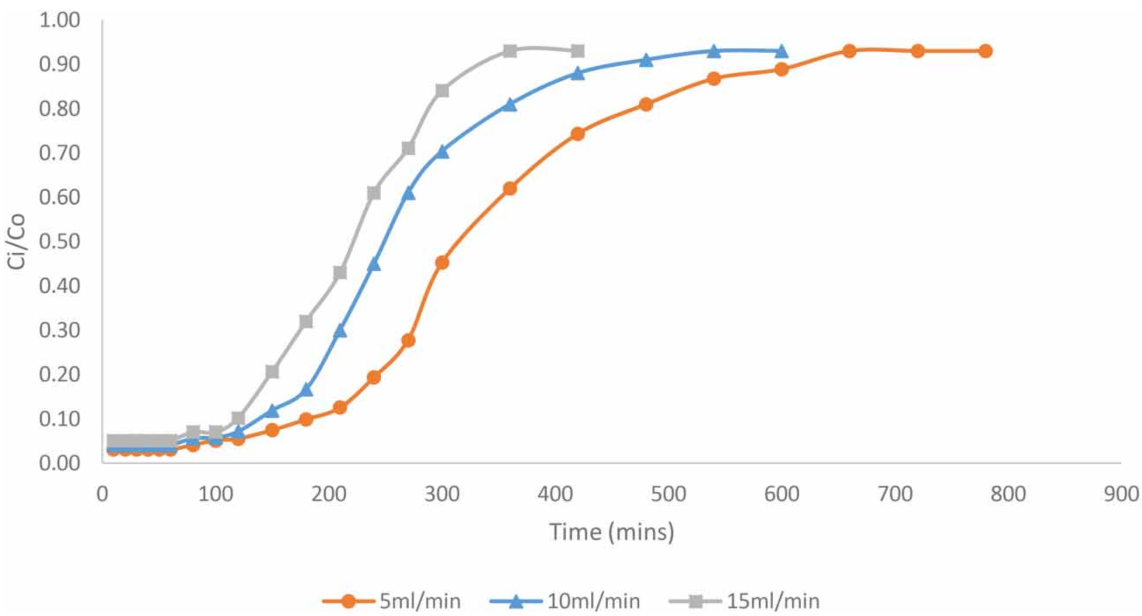

Figure 2 | Breakthrough curve COD removal by PKAC (pH = 7.3, bed-depth = 20 cm, temperature = 25 °C, inlet concentration = 421 mg L^{-1}).

steepness of the breakthrough curves as the flowrate decreases. The reason for the high breakthrough time associated with low flowrates can be due to increased contact time of the greywater with the activated carbon which results in higher removal of BOD_5 and COD. At high flowrates, the mass transfer rate increases which lead to fast saturation and this is characterized by a reduction in the slope of the curve which is an indication of a high volume of unsaturated zone due to insufficient contact time (Lopez-Cervantes *et al.* 2018). At lower flowrate, the adsorbate has more time to contact with the adsorbent and this results in high removal of adsorbate in the column (Sheng *et al.* 2018). Generally, breakthrough points occur faster with higher flowrate for both BOD_5 and COD removal. The breakthrough and exhaustion time for BOD_5 occurred faster than COD for all the flowrates studied. Results obtained in this study are in agreement with similar studies that used activated carbon from different biomasses (Ademiluyi *et al.* 2009; Nekoo & Shohreh 2013; Amale *et al.* 2014) and agricultural waste (Ghaed *et al.* 2015) to reduce BOD_5 and COD concentrations in fixed bed studies.

3.3. Effect of bed-depth on BOD_5 and COD removal

The effect of bed-depth on the breakthrough curve was studied by using three different bed-depths (10, 15, 20 cm). These were achieved by charging 15, 20 and 26 g representing 10, 15 and 20 cm respectively of the activated carbon into the column. Greywater with initial BOD_5 and COD concentrations of 252 mg L^{-1} and 421 mg L^{-1} respectively was used as feed to the fixed-bed column at a constant flowrate of 5 ml min^{-1}. The breakthrough curves for BOD_5 and COD are presented in Figures 3 and 4 respectively. As it can be seen from the shapes and

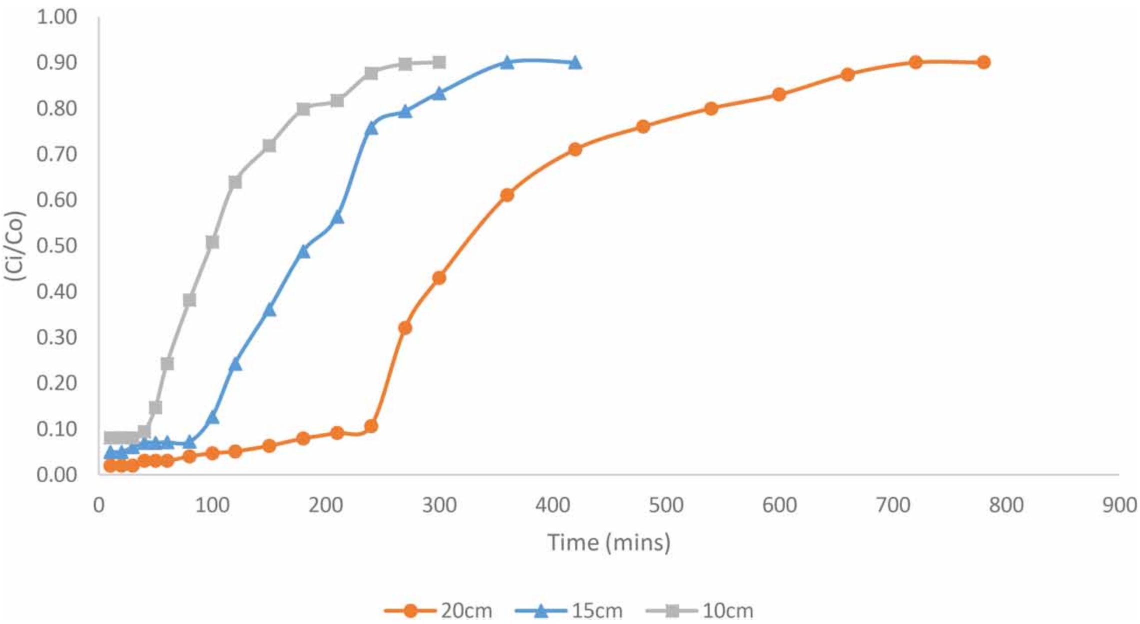

Figure 3 | Breakthrough curve and bed depth BOD_5 removal by PKAC (pH = 7.3, flowrate = 5 mL min^{-1}, temperature = 25 °C, inlet concentration = 252 mg L^{-1}).

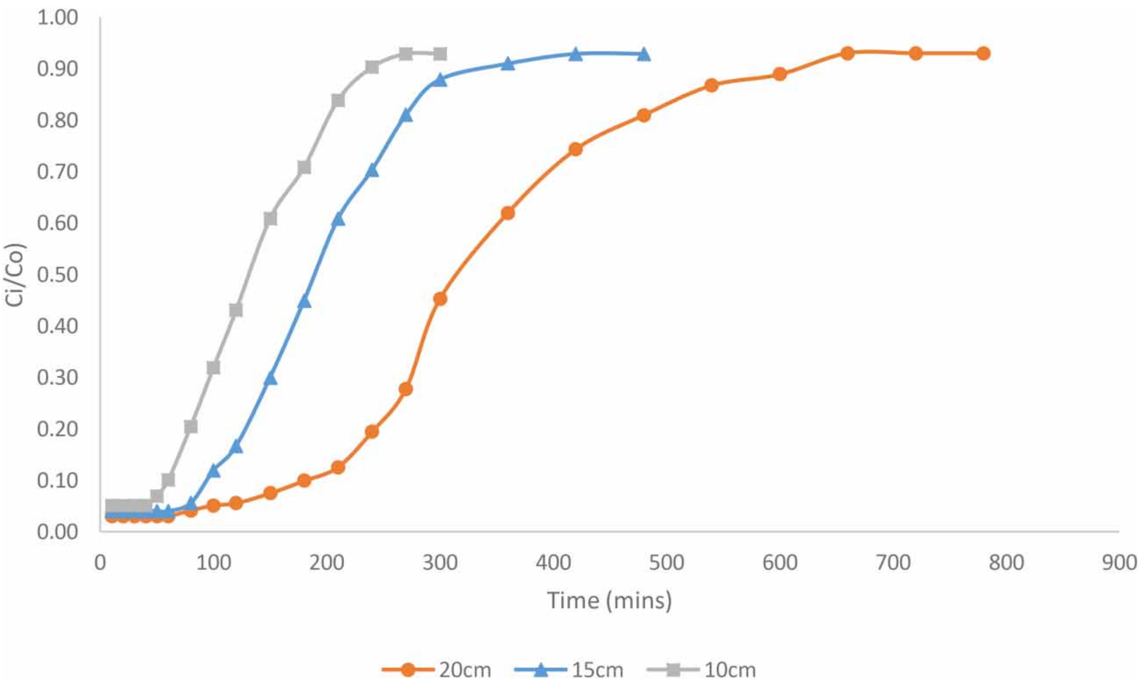

Figure 4 | Breakthrough curve and bed depth for COD removal by PKAC (pH = 7.3, flowrate = 5 mL min^{-1}, temperature = 25 °C, inlet concentration = 421 mg L^{-1}).

slopes of each curve, there are slight variations for the different bed-depths. Generally, the breakthrough time increases at higher bed-depths of the adsorbent. As the bed-depth increases from 10 to 20 cm, there is a corresponding decrease in the slope of the breakthrough curve that is observed. The breakthrough time for BOD_5 and COD also increased when the bed-depth was increased from 10 to 20 cm. This, therefore, implies that breakthrough and exhaustion times are longer with increasing bed-depth. An increase in bed-depth implies an increase in the surface area and the number of binding sites available for adsorption. This then leads to higher contact time needed for adsorption to take place as suggested by Teutscherova *et al.* (2018). The exhaustion time which is the time taken for the adsorbent to be totally used up also increased with the increase in height for both BOD_5 and COD. There was however a remarkably high exhaustion time for the 20 cm bed-depth for both BOD_5 and COD. This could be attributed to increased utilization of the bed. Generally, breakthrough time for BOD_5 is shorter than for COD for all the bed-depths studied. From the figures, it can be said that a higher bed-depth indicates a higher BOD_5 and COD can be removed due to increase in the surface area of the adsorbent, hence providing more vacant sites for adsorption to take place (Ahmad & Hameed 2010; Futalan *et al.* 2011). Other researchers have reported similar changes in breakthrough curves with changes in bed-depth using activated neem leaf powder (Patel & Vashi 2015), activated carbon from different biomasses (Ademiluyi *et al.* 2009; Nekoo & Shohreh 2013; Amale *et al.* 2014) and agriculture waste (Ghaed *et al.* 2015) to reduce BOD and COD in similar studies.

3.4. Dynamic models

3.4.1. The Thomas models

The model was applied to the experimental data under conditions of constant influent concentration, different bed-depth and different flowrates. The linearized form of the model was used to determine the Thomas rate constant (k_{TH}) and the bed capacity (q_o) of the Thomas equation for both BOD_5 and COD. The model parameters which were determined have been presented in Table 1. From the table, it can be seen that k_{Th} for BOD_5 and COD decreased with increasing bed-depth at constant flowrate, but increased with increasing flowrate at constant bed-depth. On the other hand, q_o for BOD_5 and COD increased with increase in bed-depth at constant flowrate, whereas an increase in flowrate at constant bed-depth saw a corresponding decrease in q_o. Other studies have reported similar findings in fixed-bed column (Chowdhury *et al.* 2013; Lin *et al.* 2013; Nguyen *et al.* 2015). A maximum bed capacity of 34.4 mg g^{-1} and 56.93 mg g^{-1} were obtained for BOD_5 and COD respectively at flowrate of 5 mL min^{-1} and a bed-depth of 20 cm. This maximum bed capacity was obtained at the lowest flowrate and a highest bed-depth. The maximum bed capacity occurring at this point can be due to the fact that at lower flowrates and maximum height, the adsorption capacity is high due to sufficient residence time which allows for effective utilization of the vacant sites before equilibrium is reached as suggested by Tan *et al.* (2008). A good fit ($R^2 > 0.98$) was obtained for both BOD_5 and COD as shown in Table 1. Comparing the k_{TH} between BOD_5 and COD, it can be seen that BOD_5 has a higher k_{TH} which is an indication of good column adsorption for BOD_5 as compared with COD. Comparing the q_o, it can also be seen that the q_o for COD is higher than BOD_5 indicating a higher uptake capacity of the Palm kernel activated carbon to reduce higher proportions of COD than BOD_5.

Table 1 | Thomas model parameters at different conditions

Parameter	Initial concentration (mg L^{-1})	Flowrate (mL min^{-1})	Bed height (cm)	k_{Th} (mL min-mg^{-1}) $\times 10^{-5}$	q_o (mg g^{-1})	R^2
BOD_5	252	5	10	7.18	11.13	0.92
	252	5	15	5.99	13.19	0.96
	252	5	20	3.61	34.40	0.95
	252	10	20	4.05	31.50	0.96
	252	15	20	4.92	21.26	0.95
COD	421	5	10	4.04	23.53	0.89
	421	5	15	2.92	26.41	0.88
	421	5	20	2.30	56.93	0.96
	421	10	20	2.85	49.73	0.96
	421	15	20	3.82	32.82	0.97

3.4.2. The Yoon–Nelson model

The experimental data were fitted to the Yoon–Nelson model. The linear form of the Yoon–Nelson model was used to determine the mass transfer coefficient (K_{YN}) and the time for 50% breakthrough (τ) and is presented in Table 2. Generally, as the flowrate increases at constant bed-depth, it can be seen that there is a corresponding increase in K_{YN} for BOD_5 and COD. Greater mass transfer coefficient (K_{YN}) implies narrower mass transfer zone, greater transfer coefficient between the phases and therefore lower mass transfer resistance. This implies adsorption of BOD_5 and COD is easier with higher values of K_{YN}. There is also a corresponding decrease in the time taken to reach 50% breakthrough as flowrate is increased. Brion-Roby *et al.* (2018) have reported similar changes in the Yoon–Nelson model parameters in a similar study. The changes observed can be attributed to reduced residence time associated with high flowrates. An increase in bed-depth leads to a corresponding reduction in the mass transfer coefficient but an increase in the time taken for 50% breakthrough to be achieved. This could be due to more vacant sites for adsorption to take place and hence a longer time to reach 50% of the breakthrough period. A comparatively good fit ($R^2 > 0.89$) was obtained for both BOD_5 and COD as shown in Table 2 which suggests that the Yoon–Nelson model fitted the experimental model for BOD_5 and COD in the sorption experiment.

Table 2 | Yoon–Nelson parameters at different conditions

Parameter	Initial concentration (mg L^{-1})	Flowrate (mL min^{-1})	Bed height (cm)	K_{YN} (mL min-mg^{-1}) × 10^{-2}	τ (mins)	R^2
BOD_5	252	5	10	1.81	426.66	0.92
	252	5	15	1.51	209.38	0.96
	252	5	20	0.91	521.90	0.95
	252	10	20	1.02	312.57	0.96
	252	15	20	1.24	227.48	0.98
COD	421	5	10	1.70	285.02	0.89
	421	5	15	1.71	365.89	0.96
	421	5	20	0.95	389.83	0.96
	421	10	20	1.20	295.31	0.96
	421	15	20	1.61	225.36	0.98

3.4.3. The Adams–Bohart model

The linear form of the Adams–Bohart model was applied to the experimental data by plotting C_i/C_o against *t* for both BOD_5 and COD. This model is based on surface reaction theory and assumes that equilibrium is not instantaneous therefore the adsorption rate is proportional to both the residual capacity of the adsorbent and the adsorbate concentration (Lopez-Cervantes *et al.* 2018). The values of maximum adsorption capacity (N_o) and the kinetic constant (K_{AB}) of the model have been calculated and presented in Table 3. Comparatively, the values for BOD_5 are higher than COD for all the studied conditions. The values of K_{AB} and N_o increase with an increase in flowrate for both BOD_5 and COD. Additionally, as the bed-depth is increased, the value of K_{AB} decreases while N_o increases. Similar findings have been obtained in a fixed bed column study (Brion-Roby

Table 3 | Adams–Bohart model parameters at different conditions

Parameter	Initial Concentration (mg L^{-1})	Flowrate (mL min^{-1})	Bed height (cm)	k_{AB} (mL min-mg^{-1}) × 10^{-5}	N_o (mg g^{-1}) × 10^4	R^2
BOD_5	252	5	10	3.69	.97	0.78
	252	5	15	3.45	.89	0.87
	252	5	20	2.26	1.26	0.87
	252	10	20	2.34	1.97	0.91
	252	15	20	2.62	2.34	0.88
COD	421	5	10	2.85	1.64	0.86
	421	5	15	2.40	1.46	0.87
	421	5	20	1.31	2.05	0.88
	421	10	20	1.62	3.16	0.87
	421	15	20	2.21	3.49	0.92

et al. 2018; Mondal *et al.* 2018; Xavier *et al.* 2018). The values of the $R^2 > 0.78$ recorded are lower as compared to the other models studied and thus suggests that the Adams–Bohart model would not be the best model to be used to predict the experimental data in the range of conditions used. This may be due to the fact that the Adams–Bohart model is applied in regions of low concentration and large discrepancies can be found between the experimental and predicted curve if applied outside the concentration range (Karimi *et al.* 2012).

3.4.4. The BDST model

The experimental results obtained from the column sorption experiment is fitted with the BDST model to determine the sorption capacities and kinetic constants for BOD_5 and COD. This is mostly used to predict the relationship between bed-depth (Z) of a fixed bed column and service time. The service time corresponding to bed-depth 10, 15 and 20 cm at a constant flowrate of 5 ml/l at constant inlet concentration of 252 mg L^{-1} BOD_5 and 421 mg L^{-1} COD were recorded. A plot of the service time versus bed-depths at the different bed-depth is presented in Figure 5. From the slope and intercept of Figure 5, the BDST parameters viz sorption rate constant (k), sorption capacity (N_o) and critical bed-depth (Z_o) were calculated and presented in Table 4. The high values of R^2 imply a probable linear relationship for the systems and show that the BDST model can be applied to the continuous column studies.

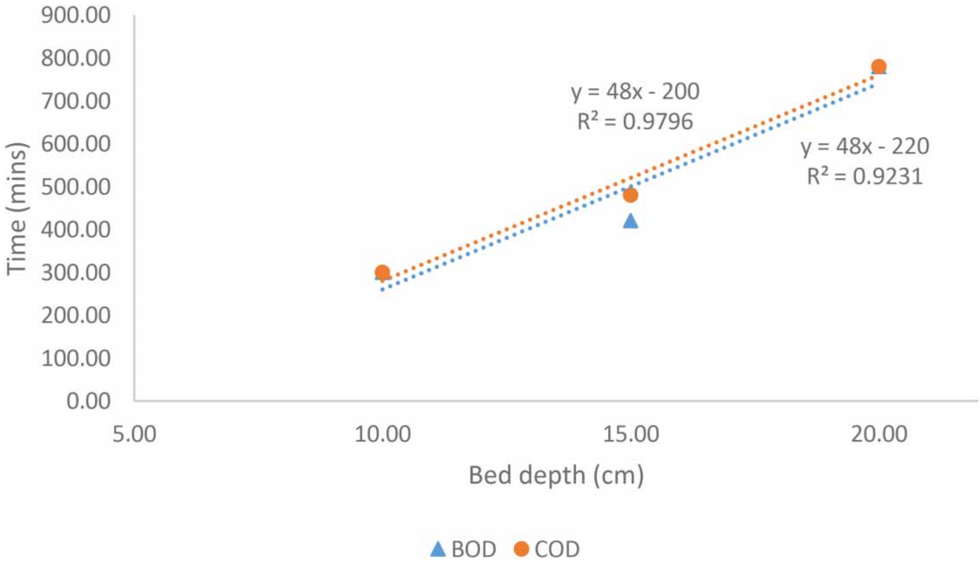

Figure 5 | Bed Depth Service Time for BOD_5 and COD.

Table 4 | BDST model parameters for BOD_5 and COD

	N_o	K_a	Z_o	R^2
BOD_5	19,353.60	3.96×10^{-5}	4.58	.92
COD	24,249.60	2.61×10^{-5}	5.56	.98

4. CONCLUSION

The removal of BOD_5 and COD from domestic greywater by sorption using PKAC was investigated in a fixed bed column under conditions of fixed inlet concentration, different inlet flowrate and different bed-depths. Based on the experimental results, PKAC has shown to be a very efficient adsorbent in the removal of BOD_5 and COD under the studied conditions. The sorption of BOD_5 and COD was strongly dependent on flowrate and bed-depth. An increase in bed-depth resulted in increased uptake capacity while an increase in flowrate resulted in a reduced uptake capacity for both BOD_5 and COD. A maximum uptake capacity of 35 mg g^{-1} and 54 mg g^{-1} was achieved for BOD_5 and COD respectively based on the Thomas model. The experimental data fitted well the Thomas, Yoon–Nelson and BDST models. The fit with Adams–Bohart model was comparatively low as compared to the other models used in this study. The Yoon–Nelson provided a better description of the experimental kinetic data in comparison to the Thomas model. This study has established the potential of using a free, locally and abundantly available waste material for the preparation of activated carbon in reducing BOD_5 and COD in domestic greywater.

ACKNOWLEDGEMENTS

The authors acknowledge funding from the Netherlands government under the NUFFIC project NICHE 194-01.

DATA AVAILABILITY STATEMENT

Data cannot be made publicly available; readers should contact the corresponding author for details.

CONFLICT OF INTEREST

The authors declare there is no conflict.

REFERENCES

Ademiluyi, F. T., Amadi, S. A., Amakama, A. & Nimisingha, J. 2009 Adsorption and treatment of organic contaminants using activated carbon from waste Nigerian bamboo. *J. Appl. Sci. Environ. Manage.* **13**, 39–47.

Ahmad, A. A. & Hameed, B. H. 2010 Fixed-bed adsorption of reactive azo dye onto granular activated carbon prepared from waste. *J. Hazard. Mater.* **175**, 298–303. doi:10.1016/j.jhazmat.2009.10.003.

Alewi, H., Obeed, W., Abdulridha, M. & Ali, G. 2021 An inquiry into the relationship between water quality parameters: biochemical oxygen demand (BOD_5) and chemical oxygen demand (COD) in Iraqi Southern region. *AIP Conf. Proc.* **2404**(1), 1–9.

Amale, P., Kulkarni, S. & Kulkarni, K. 2014 Studies on packed bed treatment for organic matter in distillery effluent. *Int. J. Eng. Sci. Innovative Technol.* **3**, 268–272.

APHA/AWWA/WEF. 2005 *Standard Methods for the Examination of Water and Wastewater*, 21st edn. American Public Health Association, American Water Works Association, Water Environmental Federation, Washington.

Bansode, R. R., Losso, J. N., Marshall, W. E., Rao, R. M. & Portier, R. J. 2004 Pecan shell-based granular activated carbon for treatment of chemical oxygen demand (COD) in municipal wastewater. *Bioresour. Technol.* **94**, 129–135. doi:10.1016/j.biortech.2003.12.009.

Behnamfard, A. & Salarirad, M. M. 2009 Equilibrium and kinetic studies on free cyanide adsorption from aqueous solution by activated carbon. *J. Hazard. Mater.* **170**, 127–133. doi:10.1016/j.jhazmat.2009.04.124.

Brion-Roby, R., Gagnon, J., Deschenes, J. S. & Chabot, B. 2018 Development and treatment procedure of arsenic-contaminated water using a new and green chitosan sorbent: kinetic, isotherm, thermodynamic and dynamic studies. *Pure Appl. Chem.* **90**, 63–77. doi:10.1515/pac-2017-0305.

Bulut, Y., Gozubenli, N. & Aydin, H. 2007 Equilibrium and kinetics studies for adsorption of direct blue 71 from aqueous solution by wheat shells. *J. Hazard. Mater.* **144**, 300–306. doi:10.1016/j.jhazmat.2006.10.027.

Chowdhury, Z. Z., Zain, S. M., Rashid, A. K., Rafique, R. F. & Khalid, K. 2013 Breakthrough curve analysis for column dynamics sorption of Mn(II) ions from wastewater by using *Mangostana garcinia* peel-based granular-activated carbon. *J. Chem.-Ny* **325**, 8–13. doi:10.1155/2013/959761.

Crini, G., Badot, P. M., Morin-Crini, N., Jolibois, B., Comte, E., Fahys, B., Gravier, E. & Torri, G. 2008 Flour of corn for dye removal from pulp and paper effluents. *Actual. Chim.*, 8–13.

Devi, R., Singh, V. & Kumar, A. 2008 COD and BOD reduction from coffee processing wastewater using avocado peel carbon. *Bioresour. Technol.* **99**, 1853–1860. doi:10.1016/j.biortech.2007.03.039.

Errais, E., Duplay, J., Darragi, F., M'Rabet, I., Aubert, A., Huber, F. & Morvan, G. 2011 Efficient anionic dye adsorption on natural untreated clay: kinetic study and thermodynamic parameters. *Desalination* **275**, 74–81. doi:10.1016/j.desal.2011.02.031.

Futalan, C. M., Kan, C. C., Dalida, M. L., Pascua, C. & Wan, M. W. 2011 Fixed-bed column studies on the removal of copper using chitosan immobilized on bentonite. *Carbohydr. Polym.* **83**, 697–704. doi:10.1016/j.carbpol.2010.08.043.

Ghaed, S., Marandi, R. & Mazhar, F. 2015 Removal of BOD_5 and COD from saline wastewater using fixed bed colum of *Aspergillus oryzae* and *Halobacillus dabanensis*. *Curr. World Environ.* **10**, 830–838.

Ghana. E. 2000 *General Environmental Quality Standards. Regulation 2000*. EPA, Ghana.

Hamdaoui, O. & Naffrechoux, E. 2007 Modeling of adsorption isotherms of phenol and chlorophenols onto granular activated carbon – part I. Two-parameter models and equations allowing determination of thermodynamic parameters. *J. Hazard. Mater.* **147**, 381–394. doi:10.1016/j.jhazmat.2007.01.021.

Han, R. P., Ding, D. D., Xu, Y. F., Zou, W. H., Wang, Y. F., Li, Y. F. & Zou, L. 2008 Use of rice husk for the adsorption of Congo red from aqueous solution in column mode. *Bioresour. Technol.* **99**, 2938–2946. doi:10.1016/j.biortech.2007.06.027.

Hidayu, A. R. & Muda, N. 2016 Preparation and characterization of impregnated activated carbon from palm kernel shell and coconut shell for CO_2 capture. *Procedia Eng.* **148**, 106–113.

Karimi, M., Shojaei, A., Nematollahzadeh, A. & Abdekhodaie, M. J. 2012 Column study of Cr (VI) adsorption onto modified silica-polyacrylamide microspheres composite. *Chem. Eng. J.* **210**, 280–288. doi:10.1016/j.cej.2012.08.046.

Kurniawan, S., Novarini, Yuliwati, E., Ariyanto, E., Morsin, M., Sanudin, R. & Nafisah, S. 2021 Greywater treatment technologies for aquaculture safety: review. *J. King Saud Univ. – Eng. Sci.* **26**, 1–8.

Lin, X. Q., Li, R. J., Wen, Q. S., Wu, J. L., Fan, J. S., Jin, X. H., Qian, W. B., Liu, D., Chen, X. C., Chen, Y., Xie, J. J., Bai, J. X. & Ying, H. J. 2013 Experimental and modeling studies on the sorption breakthrough behaviors of butanol from aqueous solution in a fixed-bed of KA-I resin. *Biotechnol. Bioprocess Eng.* **18**, 223–233. doi:10.1007/s12257-012-0549-5.

Lopez-Cervantes, J., Sanchez-Machado, D. I., Sanchez-Duarte, R. G. & Correa-Murrieta, M. A. 2018 Study of a fixed-bed column in the adsorption of an azo dye from an aqueous medium using a chitosan-glutaraldehyde biosorbent. *Adsorpt. Sci. Technol.* **36**, 215–232. doi:10.1177/0263617416688021.

Mohammad-Khah, A. & Ansari, R. 2009 Activated charcoal: preparation, characterization and applications: a review article. *Int. J. Chem. Technol.* **1**, 859–864.

Mondal, P., Mehta, D., Saharan, V. K. & George, S. 2018 Continuous column studies for water defluoridation using synthesized magnesium-incorporated hydroxyapatite pellets: experimental and modeling studies. *Environ. Processes – An Int. J.* **5**, 261–285. doi:10.1007/s40710-018-0287-6.

Nayl, A. A., Elkhashab, R. A., El Malah, T., Yakout, S. M., El-Khateeb, M. A., Ali, M. M. S. & Ali, H. M. 2017 Adsorption studies on the removal of COD and BOD from treated sewage using activated carbon prepared from date palm waste. *Environ. Sci. Pollut. R.* **24**, 22284–22293. doi:10.1007/s11356-017-9878-4.

Nekoo, S. H. & Shohreh, F. 2013 Experimental study and adsorption modelling of COD reduction in activated carbon from wastewater treatment of oil refinery Iran. *J. Chem. Chem. Eng.* **32**, 81–89.

Nguyen, A. H., Ngo, H. H., Guo, W. S., Pham, T. Q., Li, F. M., Nguyen, T. V. & Bui, X. T. 2015 Adsorption of phosphate from aqueous solutions and sewage using zirconium loaded okara (ZLO): fixed-bed column study. *Sci. Total Environ.* **523**, 40–49. doi:10.1016/j.scitotenv.2015.03.126.

Oteng-Peprah, M., de Vries, N. K. & Acheampong, M. A. 2018 Greywater characterization and generation rates in a peri urban municipality of a developing country. *J. Environ. Manage.* **206**, 498–506. doi:10.1016/j.jenvman.2017.10.068.

Oteng-Peprah, M., De Vries, N. & Acheampong, M. A. 2019 Exploring the potential of activated carbon prepared from palm kernel shell and tropical almond in BOD and COD removal from domestic greywater. In *Sustainable Wastewater mamagement; exploring the option of greywater reuse in a developing country – Ghana* (pp. 53–68). Profischen

Patel, H. & Vashi, R. T. 2012 Fixed bed column adsorption of ACID Yellow 17 dye onto tamarind seed powder. *Can. J. Chem. Eng.* **90**, 180–185. doi:10.1002/cjce.20518.

Patel, H. & Vashi, R. T. 2015 Characterization and column adsorptive treatment for COD and colour removal using activated neem leaf powder from textile wastewater. *J. Urban Environ. Eng.* **9**, 45–53.

Patel, A., Arkatkar, A., Singh, S., Rabbani, A., Solorza Medina, J. D., Ong, E. S., Habashy, M. M., Jadhav, D. A., Rene, E. R., Mungray, A. A. & Mungray, A. K. 2021 Physico-chemical and biological treatment strategies for converting municipal wastewater and its residue to resources. *Chemosphere* **282**, 130881.

Sartape, A. S., Mandhare, A. M., Salvi, P. P., Pawar, D. K. & Kolekar, S. S. 2013 Kinetic and equilibrium studies of the adsorption of Cd(II) from aqueous solutions by wood apple shell activated carbon. *Desalin. Water Treat.* **51**, 4638–4650. doi:10.1080/19443994.2012.759158.

Sheng, L. P., Zhang, Y., Tang, F. J. & Liu, S. 2018 Mesoporous/microporous silica materials: preparation from natural sands and highly efficient fixed-bed adsorption of methylene blue in wastewater. *Microporous Mesoporous Mater.* **257**, 9–18. doi:10.1016/j.micromeso.2017.08.023.

Singha, S. & Sarkar, U. 2015 Analysis of the dynamics of a packed column using semi-empirical models: case studies with the removal of hexavalent chromium from effluent wastewater. *Korean J. Chem. Eng.* **32**, 20–29. doi:10.1007/s11814-014-0183-3.

Tan, I. A. W., Ahmad, A. L. & Hameed, B. H. 2008 Adsorption of basic dye using activated carbon prepared from oil palm shell: batch and fixed bed studies. *Desalination* **225**, 13–28. doi:10.1016/j.desal.2007.07.005.

Teutscherova, N., Houska, J., Navas, M., Masaguer, A., Benito, M. & Vazquez, E. 2018 Leaching of ammonium and nitrate from Acrisol and Calcisol amended with holm oak biochar: a column study. *Geoderma* **323**, 136–145. doi:10.1016/j.geoderma.2018.03.004.

Thomas, H. C. 1944 Heterogeneous ion exchange in the flowing system. *J. Am. Chem. Soc.* **66**, 1664–1666.

TIGG, L. 2019 *Granular Activated Carbon (GAC) Media Selection*. Available from: https://tigg.com/resources/activated-carbon-knowledge-base/granular-activated-carbon-gac-media-selection/ (accessed 3 January 2019).

Xavier, A. L. P., Adarme, O. F. H., Furtado, L. M., Ferreira, G. M. D., da Silva, L. H. M., Gil, L. F. & Gurgel, L. V. A. 2018 Modeling adsorption of copper(II), cobalt(II) and nickel(II) metal ions from aqueous solution onto a new carboxylated sugarcane bagasse. Part II: optimization of monocomponent fixed-bed column adsorption. *J. Colloid Interface Sci.* **516**, 431–445. doi:10.1016/j.jcis.2018.01.068.

Yoon, Y. H. & Nelson, J. H. 1984 Application of gas adsorption kinetics; A theoretical model for respirator cartridge service time. *Am. Ind. Hyg. Assoc. J.* **45**, 509–516.

First received 2 February 2023; accepted in revised form 30 May 2023. Available online 19 June 2023